

Vibrational Analysis of Peptides, Polypeptides, and Proteins. II. β -Poly(L-alanine) and β -Poly(L-alanylglycine)

W. H. MOORE and S. KRIMM, *Harrison M. Randall Laboratory of Physics and Biophysics Research Division, Institute of Science and Technology, University of Michigan, Ann Arbor, Michigan 48109*

Synopsis

The normal vibration frequencies of poly(L-alanine) and poly(L-alanylglycine) in the antiparallel chain-pleated sheet structure have been calculated, using the force field for polyglycine I from the previous paper (*Biopolymers* 15, 2439-2464) plus additional force constants for the methyl group. The agreement with observed ir and Raman bands is very good. This substantiates the excellent transferability of the force field, since polyglycine I was shown to have a rippled-sheet structure. The amide I and amide II mode splittings are very well accounted for by transition dipole coupling, showing that subtle structural differences are sensitively manifested through this mechanism.

INTRODUCTION

The conformational structure of proteins, which are important biological molecules, can be elucidated by understanding the structure and vibrational spectra of model compounds, in particular synthetic polypeptides. This is possible because the ir and Raman spectra of poly(L-amino acids) are known to be sensitive to conformational change. In order to better correlate vibrational spectra with amino acid sequence and conformation, considerable research effort has been invested in the study of synthetic polypeptides. N-Methyl acetamide, the simplest molecule with the peptide backbone has been investigated in detail.¹⁻³ X-Ray diffraction, ir, and Raman data have also provided extensive information relevant to an understanding of the structure of more complicated polypeptides. Despite this, a detailed understanding of the vibrational spectra of polypeptides has still to be achieved.

In this paper we continue our analysis of the vibrational spectra of β polypeptides, in particular poly(L-alanine) [(Ala)_n], and poly(L-alanylglycine) [(Ala-Gly)_n]. The ir spectra of (Ala)_n in the region 3300-800 cm⁻¹ have been recorded and published.⁴ Fraser et al.⁵ have reported on the X-ray structure and ir spectra of (Ala-Gly)_n. Far ir spectra⁶⁻⁸ as well as Raman spectra from several sources^{9,10} are available on these polypeptides. These data, in conjunction with our studies on polyglycine I [(Gly I)_n]^{11,12} form the basis for the development of a transferable valence force field that

can be used to calculate and study the normal vibrational modes of β polypeptides with alkyl side chains.

The normal vibration calculations presented in this paper are based on two previously published force fields, the Jakeš and Krimm³ valence force field for the amide group and the Moore and Krimm¹² valence force field for (Gly I)_n. If force fields and associated normal vibration calculations are to be applicable in the study of tertiary structure of more complicated synthetic polypeptides and proteins, they must be systematically derived. By this we mean that the portion of the force field which describes the peptide backbone should be consistent from one polypeptide to another and essentially independent of the nature of the side chain. It is, however, necessary to consider differences in the force field that exist due to differences in residue-backbone interactions, as well as those due to the conformation of the polymer being studied. In our studies of β polypeptides we have considered only those that have alkyl side chains and whose tertiary structure is the antiparallel chain-pleated sheet, except for (Gly I)_n, which has an antiparallel chain-rippled sheet structure.¹²

For an initial force field we used the already available force field for the polyglycines^{11,12} combined with the force field for branched hydrocarbons.¹³ Available ir and Raman data for (Gly I)_n, (Ala-Gly)_n, and (Ala)_n were used as the basis for a best least squares refinement of the force field. This force field was subsequently applied in a normal vibration calculation of β -poly(L-valine) and poly(L- α -amino-*n*-butyric acid) (manuscript in preparation), and has given good agreement with experiment.

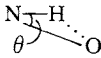
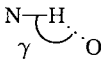
EXPERIMENTAL DATA

All of the ir and some of the Raman data used in this work were taken from the literature.⁴⁻¹⁰ The Raman data used for (Ala-Gly)_n have not been previously published, and were obtained independently in this laboratory by Hsu (unpublished results) and Johnston (unpublished results). The Johnston data were recorded on a Spex Ramalog spectrometer and cover the region from 3300 cm⁻¹ to 800 cm⁻¹. The spectrometer used by Hsu has been described elsewhere.¹⁴ These two spectra agree well; however, when discrepancies exist, values that were used in the refinement are indicated. Subsequent to the refinement, Frushour and Koenig¹⁵ published the Raman spectrum of (Ala-Gly)_n. Whenever possible their data have been incorporated.

CRYSTAL STRUCTURES

The sheet structure used for (Ala)_n was taken from the work of Arnott et al.,¹⁶ who give $a = 4.73 \text{ \AA}$ and $b = 6.89 \text{ \AA}$ (3.445 \AA per residue); the intersheet distance is $c = 5.27 \text{ \AA}$.¹⁷ As described previously,¹² the relative axial shift between two adjacent chains in the same sheet is determined from band splittings arising from transition dipole coupling. The inter-

TABLE I
Structural Parameters of Crystalline Poly(L-alanine) and Poly(L-alanyl-glycine)

		Chain Parameters	
Bond lengths (in ångström):		$r(\text{C}^\alpha\text{-C}) = 1.53$	$r(\text{C}^\alpha\text{-H}) = 1.07$
		$r(\text{C-N}) = 1.32$	$r(\text{C-H}) = 1.09$
		$r(\text{N-C}^\alpha) = 1.47$	$r(\text{N-H}) = 1.00$
		$r(\text{C=O}) = 1.24$	
Bond angles:		$\text{C}^\alpha\text{CN}[(\text{Ala})_n] = 115.4^\circ$	$\text{C}^\alpha\text{CO} = 121^\circ$
		$\text{C}^\alpha\text{CN}[(\text{Ala-Gly})_n] = 114.0^\circ$	$\text{CNH} = 123^\circ$
		$\text{CNC}^\alpha[(\text{Ala})_n] = 120.9^\circ$	
		$\text{CNC}^\alpha[(\text{Ala-Gly})_n] = 123.0^\circ$	
All angles about C^α and C^β tetrahedral			
Sheet Parameters	$(\text{Ala})_n$	$(\text{Ala-Gly})_n$	
φ	-139°	-143°	
ψ	135°	139°	
h	3.445 \AA	3.475 \AA	
$a/2$	4.73 \AA	4.71 \AA	
c	5.27 \AA	3.79 \AA (Gly) 5.08 \AA (Ala)	
α	80°	71°	
$\text{H} \cdots \text{O}$	1.76 \AA	1.74 \AA	
$\text{N} \cdots \text{O}$	2.74 \AA	2.73 \AA	
$\text{H}^\alpha \cdots \text{H}^\alpha$	2.37 \AA	2.19 \AA	
	9°	8°	
	165°	168°	

sheet organization corresponds to unit cell c of Ref. 16, where we have taken $\Delta Z = 0$, according to Colonna-Cesari et al.¹⁷

The structure used for $(\text{Ala-Gly})_n$ consists of antiparallel chain-pleated sheets in which all glycylic residues are extended from one side of the sheet and all alanyl residues from the other.⁵ The axial translation per residue is 3.475 \AA and the interchain distance within a sheet is 4.71 \AA .¹⁷ The sheets are packed such that all like residues face one another. This packing results in different sheet spacings between glycylic-glycylic and alanyl-alanyl contacts: $c(\text{Gly-Gly}) = 3.79 \text{ \AA}$ and $c(\text{Ala-Ala}) = 5.08 \text{ \AA}$.¹⁷

These and other structural parameters are collected together in Table I.

VIBRATIONAL ANALYSIS

Internal Coordinates and Corresponding Symmetry Coordinates

The conventional definitions for internal coordinates for the peptide chain are adhered to. With respect to each of the hydrogen bonds, an intermolecular $\text{H}\cdots\text{O}$ stretching coordinate, two torsion coordinates, and two bending coordinates are used: $\Delta r(\text{H}\cdots\text{O})$, $\Delta \tau(\text{C}=\text{O}\cdots\text{H})$, $\Delta \tau(\text{N-H}\cdots\text{O})$,

TABLE II
Internal Coordinates of Poly(L-alanyl-glycine) and Poly(L-alanine)

Group A	
$R_1 = \Delta r(\text{C}^\alpha\text{-C})$	$R_{16} = \Delta\theta(\text{C}^\alpha\text{-N-H})$
$R_2 = \Delta r(\text{C-N})$	$R_{17} = \Delta\theta(\text{N-C}^\alpha\text{-H})$
$R_3 = \Delta r(\text{N-C}^\alpha)$	$R_{18} = \Delta\theta(\text{N-C}^\alpha\text{-H}^\alpha)$
$R_4 = \Delta r(\text{C=O})$	$R_{19} = \Delta\theta(\text{C-C}^\alpha\text{-H})$
$R_5 = \Delta r(\text{N-H})$	$R_{20} = \Delta\theta(\text{C-C}^\alpha\text{-H}^\alpha)$
$R_6 = \Delta r(\text{C}^\alpha\text{-H})$	$R_{21} = \Delta\theta(\text{H-C}^\alpha\text{-H}^\alpha)$
$R_7 = \Delta r(\text{C}^\alpha\text{-H}^\alpha)$	$R_{22} = \Delta\gamma_{\parallel}(\text{C=O} \cdots \text{H})$
$R_8 = \Delta r(\text{H} \cdots \text{O})$	$R_{23} = \Delta\gamma_{\parallel}(\text{N-H} \cdots \text{O})$
$R_9 = \Delta r(\text{H}^\alpha \cdots \text{H}^\alpha)$	$R_{24} = \Delta\gamma_{\perp}(\text{C=O} \cdots \text{H})$
$R_{10} = \Delta\theta(\text{C}^\alpha\text{-C-N})$	$R_{25} = \Delta\gamma_{\perp}(\text{N-H} \cdots \text{O})$
$R_{11} = \Delta\theta(\text{C-N-C}^\alpha)$	$R_{26} = \Delta\omega(\text{O=C} \begin{smallmatrix} \text{N} \\ \text{C}^\alpha \end{smallmatrix})$
$R_{12} = \Delta\theta(\text{N-C}^\alpha\text{-C})$	$R_{27} = \Delta\omega(\text{H-N} \begin{smallmatrix} \text{C} \\ \text{C}^\alpha \end{smallmatrix})$
$R_{13} = \Delta\theta(\text{C}^\alpha\text{-C=O})$	$R_{28} = \Delta\tau(\text{C}^\alpha\text{-C})$
$R_{14} = \Delta\theta(\text{N-C=O})$	$R_{29} = \Delta\tau(\text{C-N})$
$R_{15} = \Delta\theta(\text{C-N-H})$	$R_{30} = \Delta\tau(\text{N-C}^\alpha)$
Group B	
$R_1 = \Delta r(\text{C}^\alpha\text{-C})$	$R_{21} = \Delta\theta(\text{N-C}^\alpha\text{-C}^\beta)$
$R_2 = \Delta r(\text{C-N})$	$R_{22} = \Delta\theta(\text{C-C}^\alpha\text{-H}^\alpha)$
$R_3 = \Delta r(\text{N-C}^\alpha)$	$R_{23} = \Delta\theta(\text{C-C}^\alpha\text{-C}^\beta)$
$R_4 = \Delta r(\text{C=O})$	$R_{24} = \Delta\theta(\text{H}^\alpha\text{-C}^\alpha\text{-C}^\beta)$
$R_5 = \Delta r(\text{N-H})$	$R_{25} = \Delta\theta(\text{C}^\alpha\text{-C}^\beta\text{-H})$
$R_6 = \Delta r(\text{C}^\alpha\text{-H}^\alpha)$	$R_{26} = \Delta\theta(\text{C}^\alpha\text{-C}^\beta\text{-H})$
$R_7 = \Delta r(\text{C}^\beta\text{-H})$	$R_{27} = \Delta\theta(\text{C}^\alpha\text{-C}^\beta\text{-H})$
$R_8 = \Delta r(\text{C}^\beta\text{-H})$	$R_{28} = \Delta\theta(\text{H-C}^\beta\text{-H})$
$R_9 = \Delta r(\text{C}^\beta\text{-H})$	$R_{29} = \Delta\theta(\text{H-C}^\beta\text{-H})$
$R_{10} = \Delta r(\text{C}^\alpha\text{-C}^\beta)$	$R_{30} = \Delta\theta(\text{H-C}^\beta\text{-H})$
$R_{11} = \Delta r(\text{H} \cdots \text{O})$	$R_{31} = \Delta\theta(\text{C=O} \cdots \text{H})$
$R_{12} = \Delta r(\text{H}^\alpha \cdots \text{H}^\alpha)$	$R_{32} = \Delta\theta(\text{N-H} \cdots \text{O})$
$R_{13} = \Delta\theta(\text{C}^\alpha\text{-C-N})$	$R_{33} = \Delta\omega(\text{O=C} \begin{smallmatrix} \text{N} \\ \text{C}^\alpha \end{smallmatrix})$
$R_{14} = \Delta\theta(\text{C-N-C}^\alpha)$	$R_{34} = \Delta\omega(\text{H-N} \begin{smallmatrix} \text{C} \\ \text{C}^\alpha \end{smallmatrix})$
$R_{15} = \Delta\theta(\text{N-C}^\alpha\text{-C})$	$R_{35} = \Delta\tau(\text{C}^\alpha\text{-C})$
$R_{16} = \Delta\theta(\text{C}^\alpha\text{-C=O})$	$R_{36} = \Delta\tau(\text{C-N})$
$R_{17} = \Delta\theta(\text{N-C=O})$	$R_{37} = \Delta\tau(\text{N-C}^\alpha)$
$R_{18} = \Delta\theta(\text{C-N-H})$	$R_{38} = \Delta\tau(\text{C}^\alpha\text{-C}^\beta)$
$R_{19} = \Delta\theta(\text{C}^\alpha\text{-N-H})$	$R_{39} = \Delta\tau(\text{C=O})$
$R_{20} = \Delta\theta(\text{N-C}^\alpha\text{-H}^\alpha)$	$R_{40} = \Delta\tau(\text{N-H})$

$\Delta\theta(\text{C=O} \cdots \text{H})$, and $\Delta\theta(\text{N-H} \cdots \text{O})$. Within the peptide group the internal coordinates for out-of-plane bending, $\Delta\omega$, are defined as in Abe and Krimm.¹¹ The definition of the coordinates associated with internal rotation follows the convention of Fukushima and Miyazawa.¹⁸ In Tables II and III we give these internal coordinates and their associated local symmetry coordinates, respectively. In these tables (Ala-Gly)_n requires both group A and B coordinates, whereas only group B coordinates are needed for a description of (Ala)_n.

TABLE III
Local Symmetry Coordinates for One Peptide Group of Crystalline
Poly(L-alanylglycine) and Poly(L-alanine)

Group A	
$S_1 = R_3$	N-C α stretch
$S_2 = R_1$	C α -C stretch
$S_3 = R_2$	C-N stretch
$S_4 = R_4$	C=O stretch
$S_5 = R_5$	N-H stretch
$S_6 = (R_6 + R_7)/2^{1/2}$	CH ₂ symmetric stretch
$S_7 = (R_6 - R_7)/2^{1/2}$	CH ₂ asymmetric stretch
$S_8 = (2R_{11} - R_{15} - R_{16})/6^{1/2}$	C-N-C α deformation
$S_9 = (5R_{12} - R_{17} - R_{18} - R_{21} - R_{19} - R_{20})/30^{1/2}$	N-C α -C deformation
$S_{10} = (2R_{10} - R_{14} - R_{13})/6^{1/2}$	C α -C-N deformation
$S_{11} = (R_{14} - R_{13})/2^{1/2}$	C=O ip bend ^a
$S_{12} = (R_{16} - R_{15})/2^{1/2}$	N-H ip bend
$S_{13} = (4R_{21} - R_{17} - R_{18} - R_{19} - R_{20})/20^{1/2}$	CH ₂ bend
$S_{14} = (R_{17} + R_{18} - R_{19} - R_{20})/2$	CH ₂ wag
$S_{15} = (R_{17} - R_{18} - R_{19} + R_{20})/2$	CH ₂ twist
$S_{16} = (R_{17} - R_{18} + R_{19} - R_{20})/2$	CH ₂ rock
$S_{17} = R_{26}$	C=O op bend ^a
$S_{18} = R_{27}$	N-H op bend
$S_{19} = R_{30}$	N-C α torsion
$S_{20} = R_{28}$	C α -C torsion
$S_{21} = R_{29}$	C-N torsion
$S_{22} = R_8$	H \cdots O stretch
$S_{23} = R_9$	H $\alpha\cdots$ H α stretch
$S_{24} = R_{22}$	C=O \cdots H ip bend
$S_{25} = R_{23}$	N-H \cdots O ip bend
$S_{26} = R_{24}$	C=O \cdots H op bend
$S_{27} = R_{25}$	N-H \cdots O op bend
Group B	
$S_1 = R_3$	N-C α stretch
$S_2 = R_1$	C α -C stretch
$S_3 = R_2$	C-N stretch
$S_4 = R_4$	C=O stretch
$S_5 = R_5$	N-H stretch
$S_6 = R_{10}$	C α -C β stretch
$S_7 = R_6$	C α -H α stretch
$S_8 = (R_7 + R_8 + R_9)/3^{1/2}$	CH ₃ symmetric stretch
$S_9 = (R_7 - R_8)/2^{1/2}$	CH ₃ asymmetric stretch 1
$S_{10} = (2R_9 - R_7 - R_8)/6^{1/2}$	CH ₃ asymmetric stretch 2
$S_{11} = (2R_{13} - R_{16} - R_{17})/6^{1/2}$	C α -C-N deformation
$S_{12} = (R_{16} - R_{17})/2^{1/2}$	C=O ip bend
$S_{13} = (2R_{14} - R_{18} - R_{19})/6^{1/2}$	C-N-C α deformation
$S_{14} = (R_{18} - R_{19})/2^{1/2}$	N-H ip bend
$S_{15} = (R_{15} + R_{21} + R_{23} - R_{20} - R_{22} - R_{24})/6^{1/2}$	N-C α -C deformation
$S_{16} = (2R_{15} - R_{21} - R_{23})/6^{1/2}$	C β bend 1
$S_{17} = (R_{21} - R_{23})/2^{1/2}$	C β bend 2
$S_{18} = (2R_{24} - R_{20} - R_{22})/6^{1/2}$	H α bend 1
$S_{19} = (R_{20} - R_{22})/2^{1/2}$	H α bend 2
$S_{20} = (2R_{28} - R_{29} - R_{30})/6^{1/2}$	CH ₃ asymmetric bend 1
$S_{21} = (R_{29} - R_{30})/2^{1/2}$	CH ₃ asymmetric bend 2

(continued)

TABLE III (continued)

$S_{22} = (2R_{25} - R_{26} - R_{27})/6^{1/2}$	CH ₃ rock 1
$S_{23} = (R_{26} - R_{27})/2^{1/2}$	CH ₃ rock 2
$S_{24} = (R_{28} + R_{29} + R_{30} - R_{25} - R_{26} - R_{27})$	CH ₃ symmetric bend
$S_{25} = R_{33}$	C=O op bend
$S_{26} = R_{34}$	N-H op bend
$S_{27} = R_{37}$	N-C α torsion
$S_{28} = R_{35}$	C α -C torsion
$S_{29} = R_{36}$	C-N torsion
$S_{30} = R_{38}$	C α -C β torsion
$S_{31} = R_{31}$	C=O · · H ip bend
$S_{32} = R_{32}$	N-H · · O ip bend
$S_{33} = R_{11}$	H · · O stretch
$S_{34} = R_{12}$	H α · · H α stretch
$S_{35} = R_{39}$	C=O torsion
$S_{36} = R_{40}$	N-H torsion

^a Here ip denotes vibrations in the plane of the amide group and op denotes vibrations out of the plane of the amide group.

Optical Activity and Selection Rules

For the optically active modes of β -(Ala)_n, the symmetry species and selection rules are those defined in Ref. 12 for the antiparallel chain-pleated sheet. There are 30 ir inactive normal modes in the *A* symmetry group, and the *B*₁, *B*₂, and *B*₃ species each have 29 ir active modes. The *B*₁ modes display parallel dichroism with respect to the chain axis, while the *B*₂ and *B*₃ modes both have perpendicular dichroism. All modes are Raman active. Crystalline (Ala-Gly)_n, with *C*₂ symmetry, has 50 and 49 normal modes of vibration in the *A'* and *A''* symmetry groups, respectively. All modes are both ir and Raman active.

Transition Dipole Coupling

Amide I Modes. In order to explain the observed splittings in amide I it is necessary to incorporate the effects of transition dipole coupling.¹² The results on (Ala)_n were obtained in conjunction with those for (Gly I)_n. As explained previously,¹² we require that from one polypeptide to another the location of the transition dipole center and its orientation with respect to the C=O bond remain unchanged. Therefore, as in (Gly I)_n, the center is 0.868 Å from the carbon atom along the C → O direction and the transition dipole is tilted 20° with respect to the C=O bond towards the N → C direction.

Using the approach described previously,¹² the change in potential energy due to two interacting transition dipoles, $\partial\mu/\partial S$, is represented by

$$\Delta V_{st} = \frac{1}{\epsilon} \left| \frac{\partial\mu_s}{\partial S_s} \right| \left| \frac{\partial\mu_t}{\partial S_t} \right| \cdot \frac{(\cos \alpha - 3 \cos \beta \cos \gamma)}{|R_{st}|^3} \Delta S_s \Delta S_t \quad (1)$$

These energy terms (in cm⁻¹) for various values of *s* and *t* represent the coefficients, *D*_{st}, in the perturbation equation:

TABLE IV
 Values of Ratios [Eqs. (3)] as a Function of Δb for Crystalline
 Poly(L-alanine) and Poly(L-alanyl-glycine)

$\Delta b, \text{ \AA}$	$(\text{Ala})_n$		$(\text{Ala})_n$: One Sheet		$(\text{Ala-Gly})_n$	
	Ratio 1	Ratio 2	Ratio 1	Ratio 2	Ratio 1	Ratio 2
0.0	-0.146	+0.854	+0.019	+1.019	-0.298	+0.702
-0.1	-0.261	+0.739	-0.090	+0.902	-0.385	+0.615
-0.2	-0.357	+0.642	-0.201	+0.799	-0.466	+0.533
-0.3	-0.439	+0.561	-0.291	+0.709	-0.534	+0.464
-0.4	-0.502	+0.487	-0.371	+0.629	-0.595	+0.404
-0.5	-0.576	+0.429	-0.442	+0.558	-0.650	+0.350
-0.6	-0.633	+0.367	-0.504	+0.496	-0.698	+0.302
-0.7	-0.687	+0.313	-0.562	+0.438	-0.745	+0.255

Observed: $(\text{Ala})_n$ —Ratio 1 = -0.40, Ratio 2 = 0.60
 $(\text{Ala-Gly})_n$ —Ratio 1 = -0.51, Ratio 2 = 0.48

$$\nu(\delta, \delta') = \nu_0 + \sum_{s,t=0}^1 D_{st} \cos(s\delta) \cos(t\delta') \quad (2)$$

where each D_{st} represents a summation over similar terms within the chosen sphere of interaction, and the D_{00} term is included in ν_0 . In order to obtain the relative axial shift between chains, we compare, as for $(\text{Gly I})_n$,¹² calculated and observed values of the following ratios:

$$\begin{aligned} \text{ratio 1} &= \frac{X_{01} + X_{11}}{X_{10} - X_{01}} = \frac{\nu(0,0) - \nu(0,\pi)}{\nu(0,\pi) - \nu(\pi,0) - 2c_1} \\ \text{ratio 2} &= \frac{X_{10} + X_{11}}{X_{10} - X_{01}} = \frac{\nu(0,0) - \nu(\pi,0) - 2c_1}{\nu(0,\pi) - \nu(\pi,0) - 2c_1} \end{aligned} \quad (3)$$

where the X 's are the geometric factors in Eq. (1).

The calculated values of the ratios, obtained from the X 's, are given in Table IV for $(\text{Ala})_n$ and $(\text{Ala-Gly})_n$. As for $(\text{Gly I})_n$,¹² the range of interaction was $\pm 35 \text{ \AA}$ within a sheet and ± 3 sheets. (For comparison, we also give the results for only one sheet of $(\text{Ala})_n$.) The observed values of the ratios, obtained from the right side of Eq. (3), will depend slightly on the value of c_1 , which is itself dependent on the force field. This constant is small, however, and, considering reasonable variations in the force field, we find that $0 \leq c_1 \leq 1.0 \text{ cm}^{-1}$; for $(\text{Ala})_n$, then, the value of ratio 1 is -0.40 and the value of ratio 2 is 0.60. This implies that $\Delta b = -0.27 \text{ \AA}$. Similarly, for $(\text{Ala-Gly})_n$ the values of ratios 1 and 2 are -0.51 and 0.48, respectively, implying that $\Delta b = -0.25 \text{ \AA}$. With these values of Δb the amide I frequencies have been calculated, and these and the interaction constants are given in Table V, with the results for $(\text{Gly I})_n$ included for comparison. It will be seen that the agreement with the observed frequencies is very good, particularly in predicting that the $\nu(0,\pi)$ frequency is almost 20 cm^{-1} higher in $(\text{Ala-Gly})_n$ than in $(\text{Gly I})_n$.

Amide II Modes. The effects of transition dipole coupling on the

TABLE V
Amide I Frequencies and Interaction Constants (in cm^{-1}) for Crystalline
Poly(L-alanine), Poly(L-alanylglycine), and Polyglycine I

	$(\text{Ala})_n$		$(\text{Ala-Gly})_n$		$(\text{Gly I})_n$	
	Obsd	Calcd	Obsd	Calcd	Obsd	Calcd
$\nu(0,0)$	1669	1669	1665	1665	1674	1674
$\nu(0,\pi)$	1695	1695	1702	1702	1685	1685
$\nu(\pi,0)$	1630	1630	1630	1630	1636	1637
$\nu(\pi,\pi)$		1701	1693	1694		1690
D_{10}		8.40		10.88		7.91
D_{01}		-24.20		-25.60		-16.10
D_{11}		11.20		6.83		10.55
D_{00}		-1.66		-3.90		-6.10
ν_0^a		1673.6		1672.9		1671.6
$\Delta\mu_{\text{eff}}^b$		0.370D		0.370D		0.348D
Δb		-0.27 Å		-0.25 Å		0.00 Å

^a $\nu_0 = \nu_0' + D_{00}$.

^b $\Delta\mu_{\text{eff}} = \tau(\partial\mu/\partial S) \Delta S$.

frequencies of the amide II vibrations in $(\text{Ala})_n$ and $(\text{Gly I})_n$ were reported previously.¹² We have also incorporated these effects into our analysis of $(\text{Ala-Gly})_n$. As in $(\text{Gly I})_n$, we have taken the center of the transition dipole moment to be along the N-H bond, 0.6 Å away from the hydrogen atom. The angle that the amide II transition moment makes with the C=O bond is similarly taken to be 68°. We calculate the magnitude of the transition dipole moment of amide II from the ratio of the intensity of the amide II band to that of the amide I band (0.532) and the effective transition moment of amide I, $\Delta\mu_{\text{eff}}$. Since amide I for $(\text{Ala})_n$ has $\Delta\mu_{\text{eff}} = 0.370\text{D}$, and this value is the same for $(\text{Ala})_n$ and $(\text{Ala-Gly})_n$, we use for amide II a $\Delta\mu_{\text{eff}} = 0.269$. The results of these transition dipole coupling calculations are given in Table VI, and agree well with observations.

Amide A and B

It has been established¹² that in the antiparallel chain-pleated sheet structure of homopolypeptides the only combinations of amide II bands that can possibly participate in Fermi resonance with the unperturbed N-H stretching mode to produce the observed amide A and amide B bands are:

$$\nu(0,0)_{\text{II}} + \nu(\pi,0)_{\text{II}} \rightarrow \nu(\pi,0)_{\text{B}} \quad (4)$$

or

$$\nu(0,\pi)_{\text{II}} + \nu(\pi,\pi)_{\text{II}} \rightarrow \nu(\pi,0)_{\text{B}} \quad (5)$$

In the previous paper¹² we showed how to calculate the unperturbed amide A and B frequencies from the frequencies and relative intensities of the observed bands. The method was applied to $(\text{Ala})_n$ and gave $\nu_a^0 = 3242$

TABLE VI
Amide II Frequencies and Interaction Constants (in cm^{-1}) for Crystalline
Poly(L-alanine), Poly(L-alanylglycine), and Polyglycine I

	(Ala) _n		(Ala-Gly) _n		(Gly I) _n	
	Obsd	Calcd	Obsd	Calcd	Obsd	Calcd
$\nu(0,0)$	1538 (R)	1534		1540	1515 (R)	1515
$\nu(0,\pi)$	1524 (ir)	1523	1535 (R, ir)	1533	1517 (ir)	1516
$\nu(\pi,0)$	1555 (R)	1555	1560 (R, ir)	1570		1563
$\nu(\pi,\pi)$		1587		1602		1588
D_{10}		-15.77		-20.60		-24.07
D_{01}		-4.95		-6.82		-6.43
D_{11}		11.04		10.34		6.13
D_{00}		-1.70		6.00		2.90
ν_0^a		1550.0		1560.8		1545.8
$\Delta\mu_{\text{eff}}^b$		0.269D		0.269D		0.254D

$$^a \nu_0 = \nu_0' + D_{00}$$

$$^b \Delta\mu_{\text{eff}} = (\partial\mu/\partial S) \Delta S.$$

and $\nu_b^0 = 3109$. Using this approach for (Ala-Gly)_n gives $\nu_a^0 = 3258$ and $\nu_b^0 = 3108$. In (Ala-Gly)_n the $\nu(\pi,\pi)$ frequency is predicted very high (1602 cm^{-1}), making the combination,

$$\nu(0,\pi)_{\text{II}} + \nu(\pi,\pi)_{\text{II}} \rightarrow \nu(\pi,0)_{\text{B}}$$

i.e.,

$$1533 + 1602 \rightarrow 3135 \text{ cm}^{-1}$$

an unlikely one for the unperturbed amide B frequency. On the other hand, the combination

$$\nu(0,0)_{\text{II}} + \nu(\pi,0)_{\text{II}} \rightarrow \nu(\pi,0)_{\text{B}}$$

i.e.,

$$1540 + 1570 \rightarrow 3110$$

agrees well with the predicted $\nu_b^0 = 3108 \text{ cm}^{-1}$.

DISCUSSION

Force Field

The force constants used to calculate the normal modes of (Ala)_n and (Ala-Gly)_n are those associated with the glycine residue, which are unchanged from the ones reported previously for (Gly I)_n,¹² plus force constants associated with the alanyl residue. The latter are given in Table VII.

No least squares refinement of N-H or C-H stretching force constants was attempted. The reported values of these force constants were adjusted to produce the best agreement with observation in (Gly I)_n, (Ala-Gly)_n, and α - and β -(Ala)_n. Modes of (Ala)_n with A, B₁, and B₂ symmetry were all

TABLE VII
 Force Constants for Alanyl Residue

Force Constant ^a	Value
1. $f(\text{C}^\alpha\text{--C}^\beta)$	4.387 ^b
2. $f(\text{N--H})$	5.674 ^c
3. $f(\text{C}^\alpha\text{--H}^\alpha)$	4.493 ^d
4. $f(\text{C}^\beta\text{--H})$	4.800 ^c
5. $f(\text{NC}^\alpha\text{C})$	0.595 ^d
6. $f(\text{NC}^\alpha\text{H}^\alpha)$	0.739 ^d
7. $f(\text{NC}^\alpha\text{C}^\beta)$	1.030 ^d
8. $f(\text{CC}^\alpha\text{C}^\beta)$	1.050 ^d
9. $f(\text{C}^\beta\text{C}^\alpha\text{H}^\alpha)$	0.642 ^d
10. $f(\text{C}^\alpha\text{C}^\beta\text{H})$	0.669 ^d
11. $f(\text{HC}^\beta\text{H})$	0.524 ^d
12. $f(\text{C}^\alpha\text{--C}^\beta \text{ tor})$	0.110 ^e
13. $f(\text{H} \cdots \text{O})$	0.150 ^c
14. $f(\text{H}^\alpha \cdots \text{H}^\alpha)$	0.011 [(Ala) _n]
15. $f(\text{H}^\alpha \cdots \text{H}^\alpha)$	0.014 [(Ala-Gly) _n]
16. $f(\text{C}^\alpha\text{C}, \text{C}^\alpha\text{C}^\beta)$	} 0.101 ^b
17. $f(\text{NC}^\alpha, \text{C}^\alpha\text{C}^\beta)$	
18. $f(\text{C}^\beta\text{H}, \text{C}^\beta\text{H})$	-0.071 ^c
19. $f(\text{C}^\alpha\text{C}, \text{NC}^\alpha\text{H}^\alpha)$	} 0.056 ^d
20. $f(\text{NC}^\alpha, \text{CC}^\alpha\text{H}^\alpha)$	
21. $f(\text{C}^\alpha\text{C}, \text{NC}^\alpha\text{C}^\beta)$	} 0.010 ^c
22. $f(\text{NC}^\alpha, \text{CC}^\alpha\text{C}^\beta)$	
23. $f(\text{C}^\alpha\text{C}, \text{CC}^\alpha\text{C}^\beta)$	} 0.417 ^b
24. $f(\text{NC}^\alpha, \text{NC}^\alpha\text{C}^\beta)$	
25. $f(\text{C}^\alpha\text{C}^\beta, \text{NC}^\alpha\text{C}^\beta)$	} 0.079 ^b
26. $f(\text{C}^\alpha\text{C}^\beta, \text{CC}^\alpha\text{C}^\beta)$	
27. $f(\text{C}^\alpha\text{C}, \text{C}^\beta\text{C}^\alpha\text{H}^\alpha)$	} 0.079 ^b
28. $f(\text{NC}^\alpha, \text{C}^\beta\text{C}^\alpha\text{H}^\alpha)$	
29. $f(\text{C}^\alpha\text{C}^\beta, \text{NC}^\alpha\text{H}^\alpha)$	} 0.217 ^d
30. $f(\text{C}^\alpha\text{C}^\beta, \text{CC}^\alpha\text{H}^\alpha)$	
31. $f(\text{NC}^\alpha, \text{NC}^\alpha\text{H}^\alpha)$	} 0.328 ^d
32. $f(\text{C}^\alpha\text{C}^\beta, \text{C}^\beta\text{C}^\alpha\text{H}^\alpha)$	
33. $f(\text{C}^\alpha\text{C}^\beta, \text{C}^\alpha\text{C}^\beta\text{H})$	} 0.100 ^d
34. $f(\text{CNC}^\alpha, \text{NC}^\alpha\text{H}^\alpha)$	
35. $f(\text{NC}^\alpha\text{C}, \text{NC}^\alpha\text{H}^\alpha)$	} -0.031 ^b
36. $f(\text{NC}^\alpha\text{C}, \text{CC}^\alpha\text{H}^\alpha)$	
37. $f(\text{NC}^\alpha\text{C}^\beta, \text{NC}^\alpha\text{H}^\alpha)$	} -0.041 ^b
38. $f(\text{CC}^\alpha\text{C}^\beta, \text{CC}^\alpha\text{H}^\alpha)$	
39. $f(\text{CC}^\alpha\text{C}^\beta, \text{C}^\beta\text{C}^\alpha\text{H}^\alpha)$	} 0.011 ^d
40. $f(\text{NC}^\alpha\text{C}^\beta, \text{C}^\beta\text{C}^\alpha\text{H}^\alpha)$	
41. $f(\text{NC}^\alpha\text{C}^\beta, \text{CC}^\alpha\text{C}^\beta)$	} 0.020 ^d
42. $f(\text{NC}^\alpha\text{C}, \text{NC}^\alpha\text{C}^\beta)$	
43. $f(\text{NC}^\alpha\text{C}, \text{CC}^\alpha\text{C}^\beta)$	} 0.310 ^d
44. $f(\text{C}^\alpha\text{NH}, \text{NC}^\alpha\text{H}^\alpha)$	
45. $f(\text{C}^\alpha\text{NH}, \text{NC}^\alpha\text{C}^\beta)$	} 0.043 ^d
46. $f(\text{NC}^\alpha\text{H}^\alpha, \text{CC}^\alpha\text{H}^\alpha)$	
47. $f(\text{NC}^\alpha\text{H}^\alpha, \text{C}^\beta\text{C}^\alpha\text{H}^\alpha)$	} -0.045 ^c
48. $f(\text{CC}^\alpha\text{H}^\alpha, \text{C}^\beta\text{C}^\alpha\text{H}^\alpha)$	
49. $f(\text{C}^\alpha\text{C}^\beta\text{H}, \text{C}^\alpha\text{C}^\beta\text{H})$	-0.045 ^c
50. $f(\text{NC}^\alpha\text{C}^\beta, \text{C}^\alpha\text{C}^\beta\text{H})^t$	-0.049 ^d

(continued)

TABLE VII (continued)

Force Constant ^a	Value
51. $f(\text{NC}^\alpha\text{C}^\beta, \text{C}^\alpha\text{C}^\beta\text{H})_g$	-0.014 ^d
52. $f(\text{C}^\alpha\text{C}^\beta\text{H}, \text{C}^\beta\text{C}^\alpha\text{H})_f$	0.122 ^d
53. $f(\text{C}^\alpha\text{C}^\beta\text{H}, \text{C}^\beta\text{C}^\alpha\text{H})_g$	0.016 ^d
54. $f(\text{N-H} \cdots \text{O})_{\text{opb}}$	0.030 ^f
55. $f(\text{C=O} \cdots \text{H})_{\text{opb}}$	0.010 ^f

^a Superscript *t*, *g* refer to *trans* and *gauche* (Ref. 13);

^b Transferred from Ref. 13 without refinement.

^c Transferred from Ref. 13 and adjusted by trial and error for agreement between observed and calculated frequencies of $(\text{Ala})_n$ (α and β) and $(\text{Ala-Gly})_n$.

^d Transferred from Ref. 13 and then refined.

^e Transferred from Ref. 25 without refinement.

^f Transferred from Ref. 11 without refinement.

used in the least squares refinement procedure. It should be noted that the value of the N-H stretching force constant required to give agreement with the unperturbed N-H stretching frequency is lower than that required for $(\text{Gly I})_n$. This is consistent with the stronger hydrogen bond in the pleated as compared to the rippled-sheet structure. As in the case of $(\text{Gly I})_n$, the interchain hydrogen bonds are not colinear with respect to the C=O and N-H bonds of the peptide groups which they connect.

A criticism of our previous force field¹¹ was that it might lack success in predicting the low-frequency modes because no account was taken of interchain interactions via $\text{H}^\alpha \cdots \text{H}^\alpha$ interactions. This argument is seemingly valid since the $\text{H}^\alpha \cdots \text{H}^\alpha$ distance in the structure of $(\text{Gly I})_n$ is only 2.6 Å, compared to a close contact of ~ 2.5 Å in crystalline polyethylene, where such interactions are known to be important.¹⁹ The $\text{H}^\alpha \cdots \text{H}^\alpha$ distances in $(\text{Ala})_n$ and $(\text{Ala-Gly})_n$ are shorter, viz., 2.37 Å and 2.19 Å, respectively, and we have therefore included such interactions in our calculations through a Williams potential.²⁰

The calculated frequencies are compared with the observed ir and Raman bands in Tables VIII and IX for $(\text{Ala})_n$ and $(\text{Ala-Gly})_n$, respectively.

Assignments

Using the observed dichroic behavior, CH_3 bending modes in $(\text{Ala})_n$ above 1410 cm^{-1} are readily assigned. In $(\text{Ala-Gly})_n$ both CH_3 and CH_2 bending modes have characteristic bands in this region. The 1447 cm^{-1} band in the Raman and ir spectra of $(\text{Ala-Gly})_n$ is most probably associated with the CH_3 and CH_2 deformations that are calculated at 1453 and 1440 cm^{-1} , respectively. In the spectra of all β polypeptides, there is a band at $\sim 1400 \text{ cm}^{-1}$, i.e., 1410 cm^{-1} in $(\text{Gly I})_n$, 1400 cm^{-1} in $(\text{Ala})_n$, and 1405 cm^{-1} in $(\text{Ala-Gly})_n$. Because in $(\text{Ala})_n$ this band is highly dichroic, we investigated the possibility of its being associated with the crystal lattice. In polypeptides with a beta carbon, the wagging of H^α is invariably the dominant contributor to the potential energy of the 1400 cm^{-1} band. However,

TABLE VIII
Observed and Calculated Frequencies (in cm^{-1}) of Poly(L-alanine)

Observed Frequencies		Calculated Frequencies			Potential Energy Distribution ^a	
Raman	Infrared	A	B ₁	B ₂		B ₃
	3242 _b	3244	3244	3244	3244	NH str(97)
		2985			2985	CH ₃ asym str 2(98)
	2985		2985		2985	
2968		2984	2984			CH ₃ asym str 1(97)
	2970 _⊥			2984	2984	
2933		2930	2930			CH ₃ sym str(99)
	2930 _⊥			2930	2930	
	2883 _⊥			2873	2883	C ^α H ^α str(97)
2871		2883	2873			
					1701	C=O str(76), CN str(13), NCC ^α def(12) C=O str(77), CN str(14), NCC ^α def(13)
1669		1669				
	1695		1695			C=O str(76), CN str(14), NCC ^α def(13) C=O str(76), CN str(13), NCC ^α def(12)
	1630 _⊥			1630		
1538		1534				NH ipb(45), CN str(30), C=O ipb(12), C ^α C str(11)
	1524		1523			NH ipb(44), CN str(30), C=O ipb(12), C ^α C str(11)
1555				1555		NH ipb(36), CN str(25), C ^α C str(17), NC ^α str(13), H ^α bend 2(10)
					1587	NH ipb(37), CN str(25), C ^α C str(17), NC ^α str(13), C=O ipb(11), H ^α bend 2(10)
		1460	1460			CH ₃ asym bend 1(63), CH ₃ rock 1(13) CH ₃ asym bend 2(75), CH ₃ rock 2(11)
		1453		1453	1453	
1451		1453				CH ₃ asym bend 2(75), CH ₃ rock 2(11) CH ₃ asym bend 2(75), CH ₃ rock 2(11)
	1455		1453			
	1446 _⊥			1450		CH ₃ asym bend 2(55), CH ₃ asym bend 1(31)
					1450	
1399		1405				H ^α bend 2(35), H ^α bend 1(18), CH ₃ sym bend(17), NC ^α str(14)
	1400		1401			
	1380 _⊥			1379	1379	CH ₃ sym bend(39), H ^α bend 1(16), H ^α bend 2(12), NH ipb(11)
1368		1363				H ^α bend 1(22), NH ipb(20), C ^α C str(17), CH ₃ sym bend(13)
			1363			
						H ^α bend 1(23), NH ipb(20), C ^α C str(17), CH ₃ sym bend(14)
	1332 _⊥		1326	1326		
1335		1329				CH ₃ sym bend(53), H ^α bend 2(25), NH ipb(12)
	1322		1329			
1311	1308			1309	1309	H ^α bend 1(49), C ^α C str(13), NH ipb(11) H ^α bend 2(30), NH ipb(19), CN str(18), C=O ipb(15)
1243	1241 _⊥			1247	1246	
1223		1228				H ^α bend 1(42), NH ipb(17), CN str(14)
	1221		1225			
1165		1168				NC ^α str(30), H ^α bend 2(27), CH ₃ rock 2(15)
	1167		1167			
				1120	1119	CH ₃ rock 2(23), NC ^α str(23), CH ₃ rock 1(12), C ^α C ^β str(10)
				1095		
1096					1095	C ^α C ^β str(42), CH ₃ rock 2(30) C ^α C ^β str(40), CH ₃ rock 2(31)
1069		1070				CH ₃ rock 1(44), C ^α C ^β str(33) CH ₃ rock 1(42), C ^α C ^β str(36)
	1050 _⊥		1069		1050	
		1046		1049		CH ₃ rock 1(43), H ^α bend 1(27) C ^α C ^β str(33), CH ₃ rock 2(21)
			1044			
		977				C ^α C ^β str(30), CH ₃ rock 2(20), CH ₃ rock 1(12) CH ₃ rock 2(37), C ^α C ^β str(19), NC ^α str(14), C ^α C str(13)
967						
	967 _⊥		978			CH ₃ rock 2(37) CH ₃ rock 1(22), CN str(12), CNC ^α def(12), C ^α C ^β str(11), C=O str(10)
909		921				
	906		913			CH ₃ rock 1(20), CN str(13), CNC ^α def(13), C ^α C ^β str(10), C=O str(12)

(continued)

TABLE VIII (continued)

Observed Frequencies		Calculated Frequencies			Potential Energy Distribution ^a
Raman	Infrared	A	B ₁	B ₂	
	926 _⊥			921	CN str(20), CH ₃ rock 2(19), NC ^α str(18), C ^α C ^β str(10)
					913 NC ^α str(23), CH ₃ rock 2(20), CN str(18), C ^α C ^β str(13)
				855	C ^α C ^β str(26), C ^α C str(23), NC ^α str(17)
				854	C ^α C str(25), C ^α C ^β str(22), NC ^α str(13), CN str(10)
				774	C ^α C (18), C=O ipb(16), CNC ^α def (14) C ^β bend 2(11), CH ₃ rock 1(11)
775	771	}			775 C=O ipb(17), C ^α C str(16), CNC ^α def(15), CH ₃ rock 1(11), C ^β bend 2(10)
		709			CN tor(33), NH opb(35), C=O opb(31), NH···O ipb(12)
	710		713		CN tor(80), NH opb(32), NH···O ipb(21)
	709 _⊥			702	699 CN tor(78), NH opb(34), NH···O ipb(20)
					C=O opb(55), CN tor(23), C ^β bend 1(10)
698		703		697	CN tor(51), C=O opb(35)
				682	C=O opb(50), NCC ^α def(13)
					682 C=O opb(53), NCC ^α def(12)
		626			C=O ipb(56), C ^α C str(15)
	622 _⊥		620		C=O ipb(57), C ^α C str(15)
	613 _⊥			624	621 NCC ^α def(40), C=O opb(19), NC ^α C def(11)
					NCC ^α def(41), C=O opb(18), NC ^α C def(11)
531	528				α-helical structure
437		425			C ^β bend 2(67), NC ^α C def(11)
	432		426		C ^β bend 2(66), NC ^α C def(10)
	445 _⊥			436	437 C ^β bend 1(50), NH opb(18)
	372				α-helical structure
375					NC ^α C def(29)
332		323			NC ^α C def(32)
	326		325		C=O ipb(35), NC ^α C def(16), CNC ^α def(15), C ^β bend 2(13)
300				300	C=O ipb(36), NC ^α C def(16), CNC ^α def(14), C ^β bend 2(14)
				298	NCC ^α def(44), C ^α C ^β tor(20), NC ^α C def(15)
266		276			NCC ^α def(43), C ^α C ^β tor(16), H···O str(10)
			287		C ^α C ^β tor(69), NC ^α C def(11)
235		240			C ^α C ^β tor(51), NC ^α C def(15)
	240		241		C ^α C ^β tor(89)
				240	C ^α C ^β tor(83), C ^β bend 2(10)
				231	C ^β bend 2(52), CNC ^α def(10)
				233	C ^β bend 2(46), C ^α C ^β tor(15), CNC ^α def(10)
			219		CNC ^α def(34), C ^α C ^β tor(51), NC ^α C def(15)
185		191			CNC ^α def(64)
				153	H···O str(54), NC ^α C def(14), NH opb(10)
			140		NH opb(40), C ^β bend 1(13), C=O opb(12)
135		139			NH opb(37), C=O opb(14), C ^β bend 1(12)
				118	NC ^α C def(23), CNC ^α def(20), NCC ^α def(11)
	122		103		NH···O ipb(23), CN tor(20), NH opb(11)
				95	NH···O ipb(29), CN tor(26), NH opb(16), C ^α C tor(14), C=O tor(12), NC ^α tor(10)
					NH opb(22), C ^β bend 1(15), H···O str(13)
91		91			H···O str(36), CNC ^α def(18)
				89	C ^α C tor(27), NC ^α tor(22), H···O str(22), CN tor(12)
			43		NH tor(29), C=O···H ipb(18), NH opb(16), NH···O ipb(10)
			35		NH tor(23), H···O str(16), C=O tor(13), NH···O ipb(13)
				31	NH···O ipb(27), NH tor(21), C=O···H ipb(19)
		25			NH tor(34), C=O···H ipb(21), C=O tor(20)

^a Only contributions 10% or greater are included.^b Unperturbed frequency.

TABLE IX
Observed and Calculated Frequencies (in cm^{-1}) of Poly(L-alanylglycine)

Observed Frequencies		Calculated Frequencies		Potential Energy Distribution ^a
Raman	Infrared	A'	A''	
	3258 ^b	{ 3248	{ 3248	NH str (96)
		{ 3248	{ 3248	
2992		2985	2985	CH ₃ asym str 1 (99)
	2978	2984	2984	CH ₃ asym str 2 (99)
2933		2930	2925	CH ₂ asym str (99)
	2925	2929	2929	CH ₃ sym str (99)
		2884		C ^α H ^α str (98)
2871			2875	
		2867		CH ₂ sym str (99)
			2863	
	1702		1703	C=O str (76), CN str (15), C ^α CN def (12)
1693		1694		
1665		1665		C=O str (77), CN str (14), C ^α CN def (12)
	1630		1630	
		1602		NH ipb (41), CN str (24), C ^α C str (15), NC ^α str (11)
1560	1560		1570	
1535	1535	1540	1533	NH ipb (47), CN str (29), NC ^α str (10)
1455		1456	1456	CH ₃ asym bend 2 (62), CH ₃ asym bend 1 (12), CH ₂ rock 2 (10)
	1450	1453	1453	CH ₃ asym bend 1 (70), CH ₃ asym bend 2 (13), CH ₂ rock 1 (10)
1447	1447	1440	1440	CH ₂ bend (98)
1404	1405	1404	1403	CH ₂ wag (31), H ^α bend 2 (18), C ^α C str (18), CH ₃ asym bend 2 (11)
1369	1371	1383	1383	CH ₃ sym bend (25), H ^α bend 1 (17), NH ipb (12), CH ₂ wag (10)
1327	1334	1330	1331	CH ₃ sym bend (62), H ^α bend 2 (22)
	~1310	1315	1315	CH ₂ wag (30), H ^α bend 1 (26)
1265	1265	1269	1271	NH ipb (32), C=O ipb (15), C ^α C str (15)
		1249		CH ₂ twist (62)
			1248	CH ₂ twist (65)
1230		1227		CH ₂ twist (25), NH ipb (18), CH ₂ wag (15), H ^α bend 1 (14), CN str (13)
	1230		1225	CH ₂ twist (23), NH ipb (18), CH ₂ wag (16), H ^α bend 1 (15), CN str (14)
1161		1163		NC ^α str (36), H ^α bend 2 (22), CH ₃ rock 2 (12)
			1163	
	1171		1163	C ^α C ^β str (43), CH ₃ rock 1 (19)
1087	~1090	1091	1091	
		1064		CH ₃ rock 2 (40), NC ^α str (16), C ^α C ^β str (12)
	~1067		1063	CH ₃ rock 2 (38), NC ^α str (20), C ^α C ^β str (20)
		1052		CH ₃ rock 1 (29), H ^α bend 1 (24), NC ^α str (19)
			1049	CH ₃ rock 1 (29), H ^α bend 1 (25), NC ^α str (18)
1004		994		CH ₂ rock (60)
	998		991	CH ₂ rock (64)
980	977			?
		958		C ^α C str (15), CN str (12)
			954	C ^α C str (17), CN str (12), NC ^α str (10), C=O str (10), C ^α C ^β str (10)
		915		CH ₃ rock 1 (19), NC ^α str (17), CN str (17), C ^α C ^β str (15)
920	920		919	CN str (22), CH ₃ rock 1 (12), NC ^α str (12), C=O str (10), CNC ^α def (10)
884		873		C ^α C str (24), CN str (16), C ^α C ^β str (11), C=O str (10)
			875	C ^α C str (21), C ^α C ^β str (15), CN str (11)
773		776		C=O ipb (18), C ^α C str (16), NC ^α C def (14), CNC ^α def (12), NC ^α str (11)
			775	C=O ipb (17), C ^α C str (18), NC ^α C def (13), CNC ^α def (13), NC ^α str (11)

(continued)

TABLE IX (continued)

Observed Frequencies		Calculated Frequencies		Potential Energy Distribution ^a
Raman	Infrared	A'	A''	
717		704		CN tor (72), NH opb (32), NH...O opb (20)
	704	701	708	CN tor (67), NH opb (32), NH...O opb (17)
		681	701	CN tor (79), NH opb (22), NH...O opb (19)
			680	CN tor (78), NH opb (38), NH...O opb (23)
			657	C=O opb (64)
			658	C=O opb (63)
			657	C=O opb (22), CN tor (13), NH opb (12)
			658	C=O opb (20), CN tor (16), NH opb (10)
630		622		C=O ipb (43), NC ^α C def (12)
	618	619		C=O ipb (47), NC ^α C def (11)
~600		573		?
554			571	C ^α CN def (28), C=O opb (28), C=O ipb (11)
432	564	423		C=O opb (30), C ^α CN def (25), C=O ipb (12)
				C ^β bend 1 (25), NC ^α C def (22), C ^β bend 2 (11), NH opb (11)
	441		423	
	370			α-helical structure
333		331		C ^β bend 2 (48), NH opb (10)
	332		335	C ^β bend 2 (42)
313		301		C ^α CN def (28), CC ^α N def (19), C=O ipb (13)
			305	C ^α CN def (29), CC ^α N def (18), C=O ipb (13)
		276		C=O ipb (25), CNC ^α def (19), NC ^α C def (13), C ^α CN def (13)
			279	C=O ipb (22), CNC ^α def (15), C ^α CN def (14), NC ^α C def (12), C ^β bend 1 (10)
	256		256	C ^α C ^β tor (32), CNC ^α def (34), H...O str (10)
		247		C ^α C ^β tor (76), CNC ^α def (14)
			230	C ^α C ^β tor (62), CNC ^α def (16)
		216		CNC ^α def (34), C ^α C ^β tor (18), C ^α CN def (16)
			189	NC ^α C def (28), CNC ^α def (23)
		187		CNC ^α def (38), NC ^α C def (21), H...O str (11)
			150	NH opb (59), C=O opb (16)
		151		NH opb (43), C=O opb (16)
		129		H...O str (74)
	110		107	CN tor (19), NH...O opb (19)
		99		NH...O opb (27), CN tor (24), NH opb (19), C ^α C tor (11)
		90		H...O str (16), NH opb (15), C ^α C tor (11)
			72	C ^α C tor (27), NC ^α tor (24), H...O str (16), NH opb (13), CN tor (11), NH...O opb (10)
			54	NH...O opb (32), NH opb (15)
		34		NH...O opb (56), C=O...H ipb (27)
			33	NH...O opb (43), C=O...H opb (30)
		25		C=O...H opb (53), NH...O opb (30)

^a Only contributions 10% or greater are included.

^b Unperturbed frequency.

in the absence of the beta carbon, as in (Gly I)_n, CH₂ wagging in conjunction with N-H in-plane bending was found to give rise to this band. In (Ala-Gly)_n, as would be expected, a combination of H^α wag and CH₂ wag contribute to a band at approximately the same frequency (1405 cm⁻¹). This absorption is also present in the α-helical form of some polypeptides, e.g., poly(L-leucine), poly(L-norleucine), and (Ala)_n. It is plausible that this particular band may be indigenous to polypeptides with aliphatic side chains and not conformationally dependent. The inclusion of the H^α...H^α intermolecular interaction causes this frequency to shift by only small amounts, viz., about 4 cm⁻¹. Because the C^α-H^α...H^α-C^α geometry has such a small effect on the frequency at ~1400 cm⁻¹, and also on all frequencies above 100 cm⁻¹, the transferability of the portion of this force field associated with

H $^{\alpha}$ and the side-chain residue to polypeptides in the α -helical form should be valid.

Elliott⁴ speculated that the observed ir band at 1308 cm⁻¹ in β -(Ala)_n was probably due to the presence of some α -helical conformation in the predominantly β sample. Actually in the ir spectrum of (Ala)_n there are two bands in this region, at 1332 and 1308 cm⁻¹.⁴ From the spectrum it is not clear if these absorptions are indeed spectral contributions from β or residual α -helical (Ala)_n. However, in the Raman spectrum of β -(Ala)_n the bands at 1335 cm⁻¹ and 1311 cm⁻¹ have intensities which are too large relative to the intensities of corresponding bands in the α form of the polymer to be assigned to residual α content. Since bands near these frequencies are predicted by our calculations, we assign the observed bands to the β form, acknowledging that there may be some contribution from the α form. In (Ala-Gly)_n, which is almost entirely in the antiparallel chain-pleated sheet structure, there are bands at 1334 cm⁻¹ (1327 cm⁻¹ in Raman) and 1310 cm⁻¹. In both polypeptides, and in both the α and β forms, these bands are associated with the CH₃ symmetric deformation and a bending motion of H $^{\alpha}$. Relatively large contributions to the potential energy from motions of the residue are consistent with the apparent conformational independence of these two bands, although some C $^{\alpha}$ -C stretching is involved in the absorption around 1311 cm⁻¹.

In (Ala)_n the amide III vibrations, which involve N-H in-plane bending and C-N stretching, account for all observed ir and Raman bands between 1200-1300 cm⁻¹. The strong and highly parallel dichroic ir absorption at 1221 cm⁻¹ is assigned to $\nu(0,\pi)$, i.e., the B_1 amide III vibration. Similarly, the 1241 cm⁻¹ ir band (1243 cm⁻¹ in the Raman), which has perpendicular dichroism, is assigned to the $\nu(\pi,0)$ (B_2) amide III mode, while the 1223 cm⁻¹ Raman band is assigned to the corresponding $\nu(0,0)$ (A) mode. As can be seen, H $^{\alpha}$ bend makes significant contributions to these modes.

It has been suggested⁹ that the Raman band at 1243 cm⁻¹ in (Ala)_n is due to the presence of the polymer in the disordered state. The normal vibration analyses of (Ala)_n and (Ala-Gly)_n, however, strongly indicate that what is observed is the splitting of amide III in the antiparallel chain-pleated sheet. The results of our subsequent calculations on poly(L-valine) also support these assignments for amide III. It is possible, of course, that the disordered polymer also has a band at 1243 cm⁻¹.

In the amide III region of (Ala-Gly)_n ir bands are observed at 1265 cm⁻¹ and 1230 cm⁻¹, and correspond to calculated frequencies at 1269 cm⁻¹ and 1225 cm⁻¹, respectively. Although the 1265 cm⁻¹ mode is predominantly N-H in-plane bend (one of the components of amide III), the 1225 cm⁻¹ band contains more of the CH₂ twisting vibration associated with the glycol residue (which predominates at 1248 cm⁻¹). Thus, this region contains significant contributions from modes other than those of the peptide group, and it therefore may not be as useful a diagnostic of the conformation of the backbone as might be expected. This conclusion is not modified by

taking interactions into account, since the calculated 1225, 1248, and 1269 cm^{-1} frequencies are insensitive to the $\text{H}^{\alpha}\cdots\text{H}^{\alpha}$ interactions.

The strong ir band at 1167 cm^{-1} in $(\text{Ala})_n$ has parallel dichroism and appears in the spectra of both α - and β - $(\text{Ala})_n$. Since the potential energy in this mode contains 30% $\text{N}-\text{C}^{\alpha}$ stretch and 27% H^{α} bend, it might seem surprising that this frequency is not more sensitive to conformation in view of the possible expectation that modes involving skeletal motions should be conformation sensitive. In fact, an examination of the eigenvectors of this vibration shows that the contribution of 15% CH_3 symmetric rock results in displacements in the $\text{C}^{\alpha}-\text{C}^{\beta}\text{H}_3$ group that predominate over those in the $\text{N}-\text{C}^{\alpha}$ bond, making this mode in a sense a side-chain mode. The situation is further complicated by the observation that in $(\text{Gly I})_n$ (which of course has no side chain) a band observed at 1162 cm^{-1} (Raman) is assignable to a mode comprised of 62% $\text{N}-\text{C}^{\alpha}$ stretch and 14% $\text{C}^{\alpha}-\text{C}$ stretch. The important point that emerges is that caution is required in assigning bands of similar frequency in different systems to similar vibrational modes.

Bands at 1096 cm^{-1} , 1050 cm^{-1} , and 909 cm^{-1} also appear in the spectra of both α - and β - $(\text{Ala})_n$. Corresponding bands appear in $(\text{Ala}-\text{Gly})_n$ spectra at ~ 1100 cm^{-1} , 1050 cm^{-1} , and 920 cm^{-1} . Since these bands are absent in the spectra of $(\text{Gly I})_n$, it is rewarding to find that all of these bands are predicted to be predominantly associated with the motion of the alanyl residue.

The dichroic character of the 771 cm^{-1} band in $(\text{Ala})_n$ is not clear. In fact from the ir spectra it is not even clear whether this band is to be identified with the β or the α form. Because in the Raman spectra of Frushour and Koenig⁹ a 775 cm^{-1} band is only observed for the rolled $(\text{Ala})_n$ fiber, which is known to be in the β form, we have assigned it to a combined $\text{C}=\text{O}$ in-plane bending and $\text{C}^{\alpha}-\text{C}$ stretching mode of the β form. Nonetheless some ir absorption at ~ 776 cm^{-1} could also be present in the α conformation, although there does not even seem to be agreement on this point.^{21,22}

In the adjustment of force constants and the assignment of bands between 695 cm^{-1} and 776 cm^{-1} for the polypeptides in the β form we again confirm the suggestion that amide V, which is due predominantly to $\text{N}-\text{H}$ out-of-plane bending and $\text{C}-\text{N}$ torsion, is confined to a small (~ 5 cm^{-1}) region around 700 cm^{-1} .²³ Although the amide V vibration near 700 cm^{-1} has been said to possess perpendicular dichroism,²³ it does not appear to be highly dichroic. We assume that the reason for this is that the amide V modes of the B_1 , B_2 , and B_3 symmetry species all contribute to the absorption near 700 cm^{-1} .

In the region from 690 cm^{-1} to 250 cm^{-1} agreement between observed and calculated frequencies is good. Two bands in β - $(\text{Ala})_n$ at 528 cm^{-1} and 372 cm^{-1} are due to the presence of some α - $(\text{Ala})_n$ in the samples. In $(\text{Ala}-\text{Gly})_n$ a band at 370 cm^{-1} is also assigned to the α -helical structure.

A recent study by Itoh and Katabuchi⁸ supports this explanation. They found that $(\text{Ala-Gly})_n$ after treatment with dichloroacetic acid assumes the α -helical conformation, as indicated by the large intensity increase in the 375–371 cm^{-1} band in conjunction with enhanced absorption at 527–523 cm^{-1} .

The bands observed near 240 cm^{-1} have previously been assigned to methyl torsion.²⁴ Using the value of the force constant associated with this assignment ($f_\tau = 0.11 \text{ m dyn-}\text{\AA}$),²⁴ the methyl torsions are well predicted at 240 cm^{-1} and 256 cm^{-1} in $(\text{Ala})_n$ and $(\text{Ala-Gly})_n$, respectively. Although these modes at $\sim 250 \text{ cm}^{-1}$ have been most often assigned to C–N torsion and referred to as amide VII, our calculations definitely indicate that this is not correct. In all molecules that contain the methyl group some absorption in the 200–260 cm^{-1} region is observed. Certainly the internal rotation around $\text{C}^\alpha\text{-C}^\beta$ in polypeptides invites a comparison with similar rotations in n -paraffins at $\sim 250 \text{ cm}^{-1}$, where a torsional force constant of $\sim 0.1 \text{ m dyn-}\text{\AA}$ is required.²⁵ Neutron scattering experiments also support this assignment.²⁶ Other aspects of the low-frequency region of the spectrum of $(\text{Ala})_n$ have been discussed in detail in the preceding paper.¹²

CONCLUSIONS

It is seen that the force field transferred from $(\text{Gly I})_n$,¹² to which constants associated with the methyl group have been added, provides a very good prediction of the vibrational spectra of $(\text{Ala})_n$ and $(\text{Ala-Gly})_n$ in the antiparallel chain-pleated sheet structure. Since $(\text{Gly I})_n$ has a rippled-sheet structure,¹² this force field exhibits a high degree of transferability for β polypeptides.

As for $(\text{Gly I})_n$,¹² transition dipole coupling is important in accounting for the splittings in the amide I and amide II modes. The incorporation of this interaction mechanism also permits the determination of the axial shift, Δb , between chains in a sheet, probably more sensitively than is possible at present by X-ray or electron diffraction techniques on such poorly ordered systems. It is interesting to note that Δb is in the range of -0.25 to -0.45 \AA for the pleated sheet (based also on our calculations of other β polypeptides), whereas for the rippled sheet of $(\text{Gly I})_n$ we find that $\Delta b \cong 0$.¹² Despite these structural differences, the unperturbed peptide group amide I frequency is essentially the same in all β structures, $\sim 1673 \text{ cm}^{-1}$. The unperturbed amide II frequency is not nearly so constant, reflecting the less localized character of this mode.¹²

While the amide I and amide II modes are very characteristic of the main-chain conformation, we see that this is not as true of bands in the amide III region. The reason for this is that modes in this region (1200–1300 cm^{-1}) contain significant side-chain contributions. Caution is therefore called for in using this region for diagnostic purposes.

Subsequent papers in this series will consider the analysis of the vibrational spectra of other β polypeptides as well as polypeptides in other conformations. The analysis of small peptides as well as proteins will also be discussed.

This work was supported by National Science Foundation Grants BMS74-21163 and MPS75-05239.

References

1. Miyazawa, T., Shimanouchi, T. & Mizushima, S. (1958) *J. Chem. Phys.* **29**, 611–616.
2. Itoh, K. & Shimanouchi, T. (1967) *Biopolymers* **5**, 921–930.
3. Jakeš, J. & Krimm, S. (1971) *Spectrochim. Acta* **27A**, 19–34.
4. Elliott, A. (1954) *Proc. Roy. Soc., Ser. A* **226**, 408–421.
5. Fraser, R. D. B., MacRae, T. P., Stewart, F. H. C. & Suzuki, E. (1965) *J. Mol. Biol.* **11**, 706–712.
6. Itoh, K., Nakahara, T., Shimanouchi, T., Oya, M., Uno, K. & Iwakura, Y. (1968) *Biopolymers* **6**, 1759–1766.
7. Itoh, K., Shimanouchi, T. & Oya, M. (1969) *Biopolymers* **7**, 649–658.
8. Itoh, K. & Katabuchi, H. (1972) *Biopolymers* **11**, 1593–1605.
9. Frushour, B. G. & Koenig, J. L. (1972) *Biopolymers* **13**, 455–474.
10. Fanconi, B. (1973) *Biopolymers* **12**, 2759–2776.
11. Abe, Y. & Krimm, S. (1972) *Biopolymers* **11**, 1817–1839.
12. Moore, W. H. & Krimm, S. (1976) *Biopolymers* **15**, 2439–2464.
13. Schachtschneider, J. H. & Snyder, R. G. (1964) *J. Polym. Sci., Part C* **7**, 99–124.
14. Hsu, S. L., Moore, W. H. & Krimm, S. (1975) *J. Appl. Phys.* **46**, 4185–4193.
15. Frushour, B. G. & Koenig, J. L. (1975) *Biopolymers* **14**, 2115–2135.
16. Arnott, S., Dover, S. D. & Elliott, A. (1967) *J. Mol. Biol.* **30**, 201–208.
17. Colonna-Cesari, F., Premilat, S. & Lotz, B. (1975) *J. Mol. Biol.* **95**, 71–82.
18. Fukushima, K. & Miyazawa, T. (1965) *J. Mol. Spectrosc.* **15**, 308–318.
19. Tasumi, M. & Krimm, S. (1967) *J. Chem. Phys.* **46**, 755–766.
20. Williams, D. E. (1967) *J. Chem. Phys.* **47**, 4680–4684.
21. Itoh, K. & Shimanouchi, T. (1970) *Biopolymers* **9**, 383–399.
22. Fanconi, B., Small, E. & Peticolas, W. (1971) *Biopolymers* **10**, 1277–1298.
23. Masuda, Y., Fukushima, K., Fujii, T. & Miyazawa, T. (1969) *Biopolymers* **8**, 91–99.
24. Moore, W. H., Ching, J. H. C., Warrier, A. V. R. & Krimm, S. (1973) *Spectrochim. Acta* **29A**, 1847–1858.
25. Moore, W. H. & Krimm, S. (1973) *Spectrochim. Acta* **29A**, 2025–2042.
26. Drexel, W. & Peticolas, W. L. (1975) *Biopolymers* **14**, 715–721.

Received May 10, 1976

Accepted July 12, 1976